Small crystal approach for the electronic properties of double-wall carbon nanotubes

2009 New J. Phys. 11 043002

(http://iopscience.iop.org/1367-2630/11/4/043002)

New Journal of Physics
The open-access journal for physics

Small crystal approach for the electronic properties of double-wall carbon nanotubes

Jessica Alfonsi and Moreno Meneghetti
Department of Chemical Sciences, University of Padova,
Via Marzolo 1, 35131 Padova, Italy
E-mail: moreno.meneghetti@unipd.it

New Journal of Physics **11** (2009) 043002 (13pp)
Received 16 November 2008
Published 1 April 2009
Online at http://www.njp.org/
doi:10.1088/1367-2630/11/4/043002

Abstract. A small crystal approach (SCA) is a real-space approach that allows one to introduce local symmetry breaking which is difficult to consider in a reciprocal space approach. We apply the SCA to the case of double-wall nanotubes, for which the effects of the orientation-dependent intertube interactions have to be taken into account. The results suggest a solution for the usual difficulties in assigning the resonance Raman spectra of double-wall nanotubes since important variations of the electronic spectra of these carbon nanotubes are found with respect to those of the constituent single-wall nanotubes.

Contents

1. Introduction

Since the discovery of multi-wall carbon nanotubes (MWNTs) in 1991 by Iijima [1] and the following synthesis of single-wall nanotubes (SWNTs) [2], considerable effort has been devoted to the theoretical investigation of the optoelectronic properties of these systems [3, 4]. One of the important aims at the basis of this effort is to provide an interpretative tool for the available experimental measurements provided by resonance Raman spectroscopy (RRS) and photoluminescence (PL) [5]–[7]. The excitonic nature of the optical spectra of SWNTs [8, 9] has been addressed in recent years [10]–[15] (see section 3.7 and references therein in [16]), but many experimental RRS and PL results are also successfully interpreted, with reasonable approximation, by semiempirical tight-binding (TB) calculations ([3], [17] and references therein). This has been related to the opposite effects, on the electronic energies, of the electronic correlation and of the excitonic interaction together with the one-dimensional structure of nanotubes (NTs) and the related van Hove singularities (vHs) [18].

A reciprocal space approach like that followed by the usual TB approach finds, however, difficulties for problems in which local symmetry is broken like in the case of functionalization, doping and other disorder effects such as interactions among NTs and with the surrounding environment. For instance, the solution of the TB Hamiltonian in reciprocal space for the simplest form of MWNTs, i.e. double-walled nanotubes (DWNTs), was obtained only for a restricted number of NT geometries with higher symmetry [19]–[22].

Using a real-space representation one can understand symmetry breaking effects due to defects and/or other interactions in the ideal NT system in a simple way since local effects can be directly introduced. A real-space approach has been considered with models for transport properties [23]. However, the translational periodicity of the NT, which is important for the computation of optical properties, was not introduced. In this work, we use a real-space approach, called the *small crystal approach* (SCA) ([24], [25] and references therein), to sample the points of the NT Brillouin zone (BZ) which determine vHs in the density of states (DOS). This allows us to calculate the optical absorption spectra of NTs, and in particular of DWNTs, for which the interaction of the two NTs cannot be fully considered in a reciprocal space approach. The results show important symmetry breaking effects on the electronic spectrum of the DWNT with respect to that of the constituent tubes which suggests that the RRS and PL spectra of these NTs cannot be simply understood on the basis of the electronic spectra of the constituent tubes, as is usually done.

2. SCA for the optical properties of CNTs

The SCA considers a small number of unit cells with appropriate boundary conditions to calculate the electronic states only at some selected points of the first BZ. For a SWNT, we can use, in the simplest case, one unit cell with periodic boundary conditions (PBCs). In this case the cluster samples the centre of the 1D NT BZ, for each of the $2N$ bands labelled by the azimuthal quantum number index μ, where $2N$ is the number of atoms in the unit cell. In figure 1, we report the cutting lines of the reciprocal space of the (5, 0) NT superimposed on the graphene hexagonal reciprocal space structure. The points sampled by a unit cell with PBCs are those at $k_z = 0$. One can follow two ways to sample more and/or other points within the 1D BZ. In the first case, one can use a super-cluster including U translational unit-cells. In this case

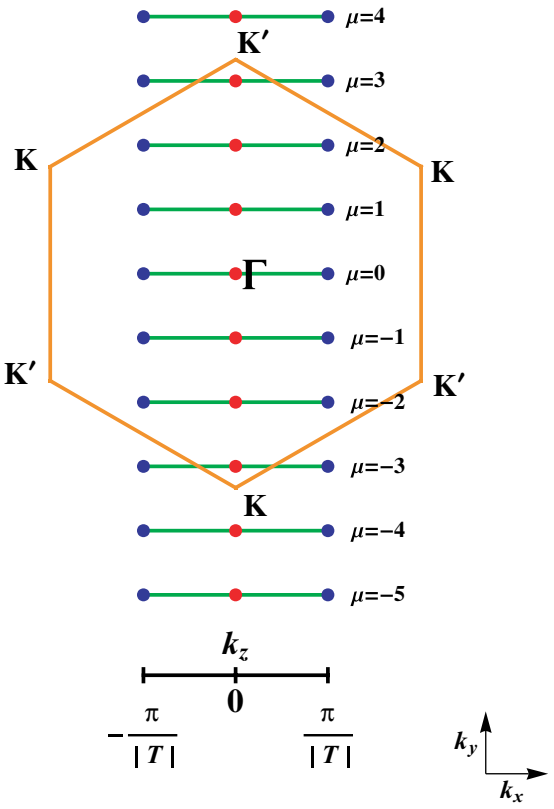

Figure 1. NT BZ of (5, 0) tube superimposed on the 2D graphene BZ: points sampled with one unit-cell cluster and PBCs are shown as red dots. Additional points (blue dots) at the edges of each 1D BZ are sampled with a two unit-cell cluster and PBCs.

one samples k-states at

$$\left(\mu, k_z = \pm\frac{2\pi\kappa}{UT}\right) \quad \text{with} \quad \kappa = 0, \ldots, U-1, \tag{1}$$

where T is the norm of the translation unit vector $\mathbf{T} = (2m+n)/d_R\mathbf{a}_1 - (2n+m)/d_R\mathbf{a}_2$, $\mathbf{a}_1$ and $\mathbf{a}_2$ are the unit vectors of the graphene lattice and the integer d_R is the greatest common divisor of $2m+n$ and $2n+m$ with n and m the chiral indices of the NT.

In the second case one can multiply the Hamiltonian matrix elements, related to periodic axial boundary conditions, by a complex exponential factor of period 2π

$$h_{i,j} = \tilde{h}^*_{j,i} = t_\pi \exp(\mathrm{i}\phi) \quad \text{with} \quad -\pi \leqslant \phi \leqslant \pi, \tag{2}$$

where t_π is the hopping parameter. In this case one can study points at $k_z = \pm\pi/nT$ using $\phi = \pm\pi/n$. For example, points at $k_z = \pm\pi/T$ are sampled by applying a phase $\phi = \pm\pi$. This kind of condition is called *antiperiodic boundary conditions* (APBCs), while the previously employed PBC implies $\phi = 0$. Figure 1 shows the points of the first BZ sampled by using PBC (red points) or APBC (blue points) for the (5, 0) NT. By changing ϕ over the full 2π range within the 1D BZ, as indicated in equation (2), the π-TB electronic dispersion relation from the zone-folding (ZF) method is completely recovered for a given (n, m) NT. In figure 2, we show the calculation obtained with $t_\pi = 2.9$ eV, which is considered appropriate for

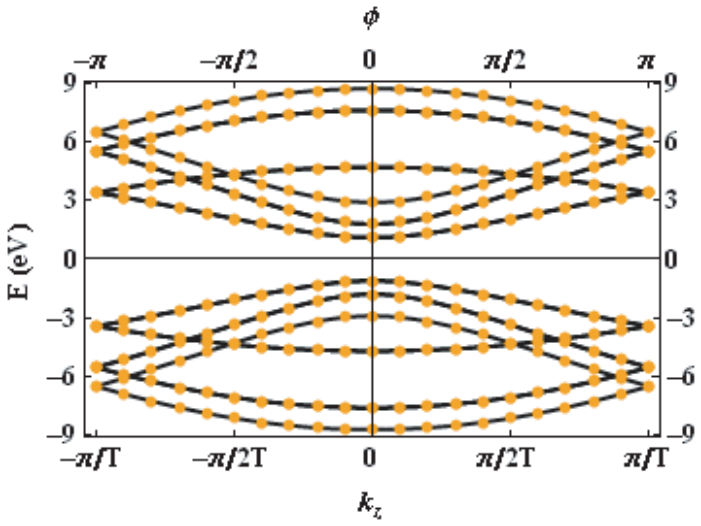

Figure 2. Band structure of (5, 0) calculated by SCA (orange dots) superimposed on the ZF electronic dispersion (black lines).

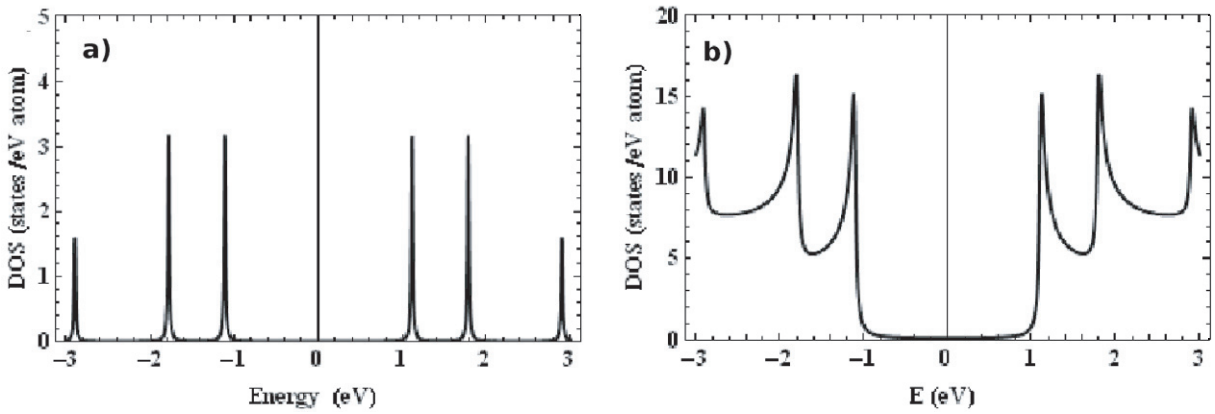

Figure 3. DOS of (5, 0) tube calculated by (a) SCA including only $k_z = 0$ points and (b) full BZ integration of ZF dispersion relation.

SWNTs [3, 26] and will be used also in the following. In general, the whole first BZ has to be considered for the accurate prediction of the electronic properties of the system. However, not all the k-points contribute significatively. In the case of SWNTs the optical spectra are dominated by the vHs in the DOS which are found at the extrema of the dispersion curves [3, 4]. For example, looking at the plot of the energy dispersion of zigzag CNTs, the states giving vHs in the DOS are found at the centre of the 1D BZ, i.e. $k_z = 0$. Figure 3 shows, as an example, the comparison between the DOS obtained by the ZF scheme and that obtained by considering only the $k_z = 0$ points sampled with the SC approach, for the zigzag NT (5, 0). One can see that the two results show the same relevant features, as expected. Therefore, one can predict that also the optical properties can be accounted for by this approach if the sampled points include those determining the vHs. As an example, we calculate the optical properties of zigzag NTs.

The transition dipole vector [16], [27]–[31] is

$$\begin{aligned}\mathbf{D} &= \langle \Psi^c | \nabla_z | \Psi^v \rangle \\ &= \sum_{h=0}^{N-1} \sum_{l=1,3} \sum_{s'=A,B} c^*_{l,s'} \sum_{s=A,B} c_{h,s} \langle \phi_z(r - \mathbf{R}_{l,s'}) | \nabla_z | \phi_z(r - \mathbf{R}_{h,s}) \rangle, \end{aligned} \tag{3}$$

where the index $l = 1, 2, 3$ labels the interatomic vectors $r^l_{h,s} = \mathbf{R}_{l,s'} - \mathbf{R}_{h,s}$ pointing from one site $s = A(B)$ in the hth graphene cell to each of the three nearest neighbours $B(A)$ and $c_{h,s}$ define the contributions of the p_z-like atomic orbitals $\phi_z(r - \mathbf{R}^u_{h,s})$ to the wavefunctions. The matrix element between $\phi_z(r - \mathbf{R}^u_{h,s})$ is written as [16], [27]–[29]

$$\left\langle \phi_z \left(r - \mathbf{R}_{l,s'}\right) | \nabla_z | \phi_z \left(r - \mathbf{R}_{h,s}\right) \right\rangle = M_{\text{opt}} \frac{a}{\sqrt{3}} r^l_{h,s}, \tag{4}$$

where M_{opt} is the atomic dipole transition matrix element, parallel to the interatomic vector $r^l_{h,s}$ and evaluated at the first nearest-neighbour distance $a_{CC} = 0.142$ nm. As a first approximation, M_{opt} can be considered a constant that normalizes the resulting values of the dipole matrix elements [16, 27, 32, 33]. Developing the summation over s and s' in terms of the contribution to the dipole matrix element from A-sites to B-sites and vice versa, we obtain

$$D_z = \frac{a M_{\text{opt}}}{2\sqrt{3}} \left[\sum_{h=0}^{N-1} \sum_{l=1,3} c^*_{l,B} c_{h,A} \left(r^l_{h,A}\right)_z + \sum_{h=0}^{N-1} \sum_{l=1,3} c^*_{l,A} c_{h,B} \left(r^l_{h,B}\right)_z \right], \tag{5}$$

where the projection along the tube axis z has been considered, since it is known that the transition with the dipole moment perpendicular to the axis is strongly suppressed by the antenna effect [34, 35]. The selection rules for vertical transitions involving a given $(\mu, k_z = 0)$ valence band state and another $(\mu', k_z = 0)$ conduction band state are automatically obtained through equation (5):

$$\begin{aligned} &\delta_{\mu,\mu'} = 0 \Longrightarrow D_z = 0, \\ &\delta_{\mu,\mu'} = 1 \wedge (\mu, \mu' \neq 0) \Longrightarrow D_z \neq 0, \end{aligned} \tag{6}$$

in accord with the ZF selection rules [16], [27]–[29].

The calculation of the optical absorption spectrum can be obtained by the sum over states (SOS) method [36]. In figure 4, we compare the optical absorption spectrum of the periodic zigzag cluster (5, 0) based on a SC approach calculation, where a Lorentzian function is used for each resonance, to that obtained with the ZF approach. The results show that the same fundamental features (transition energies and relative intensities of the transitions) are obtained. Therefore, one concludes that the optical properties of NTs can be obtained with a small cluster and appropriate boundary conditions if they allow sampling of the vHs of the first BZ.

3. Optical properties of DWNTs

Carbon DWNTs are interesting systems because their structure can be considered that of a SWNT protected by the external SWNT on which functionalization can be operated without affecting the properties of the internal tube [37, 38]. They can be commensurate if the ratio of the translational periods of the constituent SWNTs is a rational number. According to this definition, DWNTs with both armchair or zigzag NTs are always commensurate, while

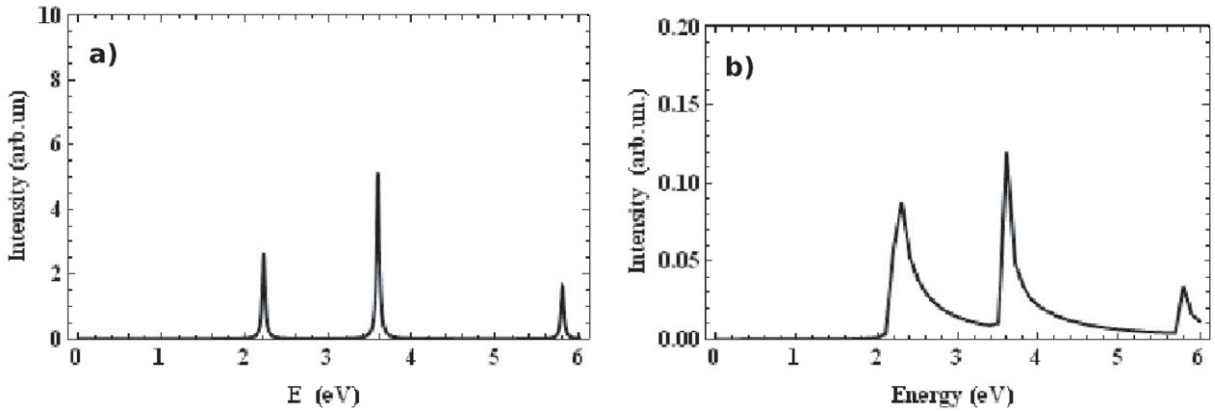

Figure 4. Optical absorption intensity of a (5, 0) tube calculated by (a) SCA including only $k_z = 0$ points and (b) full BZ integration of ZF dispersion relation.

a DWNT with a zigzag tube inserted into an armchair one is incommensurate [39]. As recalled in the introduction, besides PL, RRS allows to characterize the NTs present in a sample by assigning their radial breathing modes (RBM). The assignment is based on calculated Kataura plots [6] that correlate SWNT electronic excitations with their diameters. A similar route was also attempted, without complete success, for DWNTs [40, 41], with the basic assumption that these systems can be modelled as two almost non-interacting SWNTs. Based on this assumption, the electronic structure of a DWNT is simply the sum of the electronic structures of the constituent tubes. Perturbative effects due to weak intertube electronic coupling are considered negligible or at least responsible for a slight shift on the single-particle transition energies around the Fermi level. By applying the SC approach to DWNTs, we will show that this picture is only partially correct and that new transitions can be expected originating from the symmetry breaking of the band degeneracies, in particular in the visible range. Moreover, we will show that different mutual orientations between the concentric NTs due to azimuthal rotation or translation parallel to the DWNT axis can significatively alter the absorption spectra. To show the new features appearing in the electronic spectrum, we choose to consider DWNTs obtained with zigzag NTs for which the cluster and the boundary conditions to study the relevant electronic states are simpler, as recalled in the previous sections, but the calculations can be done for all other types of NTs as well. Furthermore, among all possible ways to combine SWNTs into DWNTs, we consider those with an interlayer distance between 0.334 nm (graphite interlayer spacing) and 0.360 nm, as was experimentally found [42]. For zigzag DWNTs, we find in this interval all combinations of type $(n, 0)@(n', 0)$ such that $n - n' = 9$ which have an interlayer of 0.352 nm, for CC bond length of 0.142 nm. We consider in our examples a semiconductor–semiconductor (S–S) DWNT, such as (5, 0)@(14, 0) and a metallic–metallic (M–M) one, such as (9, 0)@(18, 0). The TB Hamiltonian for a DWNT can be written as a sum of the TB Hamiltonians corresponding to the inner and outer NTs plus a perturbative term H_{inter} for the electronic hopping from a site l on the inner tube to another site m on the outer tube. The intertube interaction is considered to decay exponentially with the distance $d_{l,m}$ between the sites, according to the parametrization first introduced by Roche *et al* [43] for these systems:

$$H_{\text{INTER}} = \beta_\pi \sum_{\langle l,m\rangle,\sigma}^{\text{out,in}} \cos\theta_{l,m} \exp\left[\left(d_{l,m} - \Delta\right)/\delta_\pi\right]\left(c^\dagger_{l,\sigma} c_{m,\sigma} + c_{l,\sigma} c^\dagger_{m,\sigma}\right). \tag{7}$$

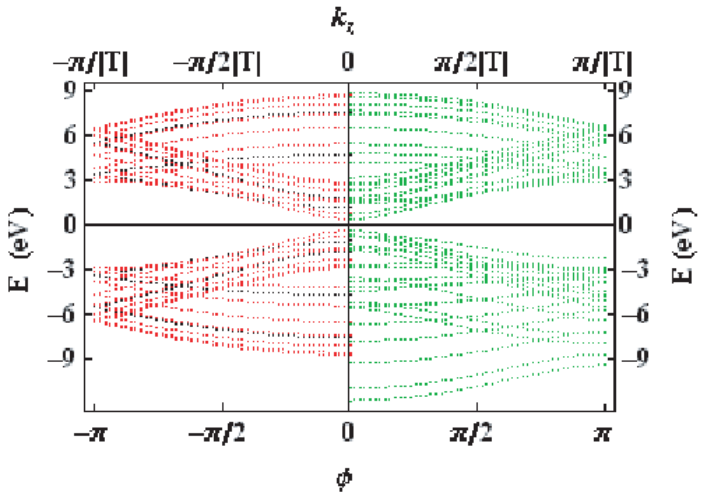

Figure 5. Electronic band structure of (5, 0)@(14, 0) DWNT at default configuration ($\phi = 0$, $\Delta Z = 0$) with non-interacting constituent SWNTs (left panel) and with intertube hopping (right panel, $\beta_\pi = 1.0$ eV). Colour legend: black (inner SWNT), red (outer SWNT), green (DWNT with interaction on).

In the above expression for H_{INTER}, Δ is the interlayer spacing (semidifference between diameters), δ_π is the decay constant for π orbitals, $\theta_{l,m}$ is the angle between π orbitals pointing perpendicularly to the tubes' surface and β_π is the intertube hopping amplitude integral. According to the literature, values for β_π can range from $t_\pi/8$ to 1.0 eV and $\delta_\pi = 0.045$ nm [43]–[45] according to *ab initio* results for turbostratic graphite [21, 46, 47].

Intertube hopping interaction depends, therefore, on the mutual orientation of the constituent coaxial SWNTs, namely on the azimuthal angle $\Delta\Phi$ and the translation ΔZ parallel to the tube axis. Therefore, we can write

$$\theta_{l,m} \equiv \theta_{l,m}(\Delta\Phi), \qquad d_{l,m} \equiv d_{l,m}(\Delta\Phi, \Delta Z).$$

In figure 5, the electronic dispersion relation for the considered DWNTs are shown for the default configuration ($\Delta\Phi = 0$, $\Delta Z = 0$) using $\beta_\pi = 1.0$ eV. The main effect of H_{INTER} is the lifting of the doubly degenerate bands and the breaking of the symmetry of valence and conduction bands with respect to the Fermi level. This is more evident far from the Fermi level and is stronger for valence bands than for conduction bands. We now consider how the total π electronic energy varies as a function of the orientational parameters, namely the azimuthal shift $\Delta\Phi$ and the translational shift ΔZ. Figure 6 shows some results obtained by summing to convergence the energy of the states sampled over the entire BZ. One observes in figure 6(c) and (d) two minima around $\Delta Z = \pm A/4$ (in zigzag NTs $A = |T| = 0.426$ nm) using $\Delta\Phi = 0$ for (5, 0)@(14, 0) and $\Delta\Phi = \pi/36$ for (9, 0)@(18, 0) (figures 6(c) and (d)). On the other hand, the dependence on $\Delta\Phi$, at $\Delta Z = A/4$ (figures 6(a) and (b)), shows a periodic oscillatory behaviour, with an energy minimum located at $\Delta\Phi = \pi/36$, only for (9, 0)@(18, 0). These results agree with those obtained by symmetry arguments by Damnjanović *et al* [39, 48], although in this case one appreciates that the minima are small minima, in particular in the case of the dependence on $\Delta\Phi$. In the following calculations, we will use $\Delta Z = A/4$ for both DWNTs and $\Delta\Phi = 0$ and $\pi/36$ for (5, 0)@(14, 0) and (9, 0)@(18, 0), respectively.

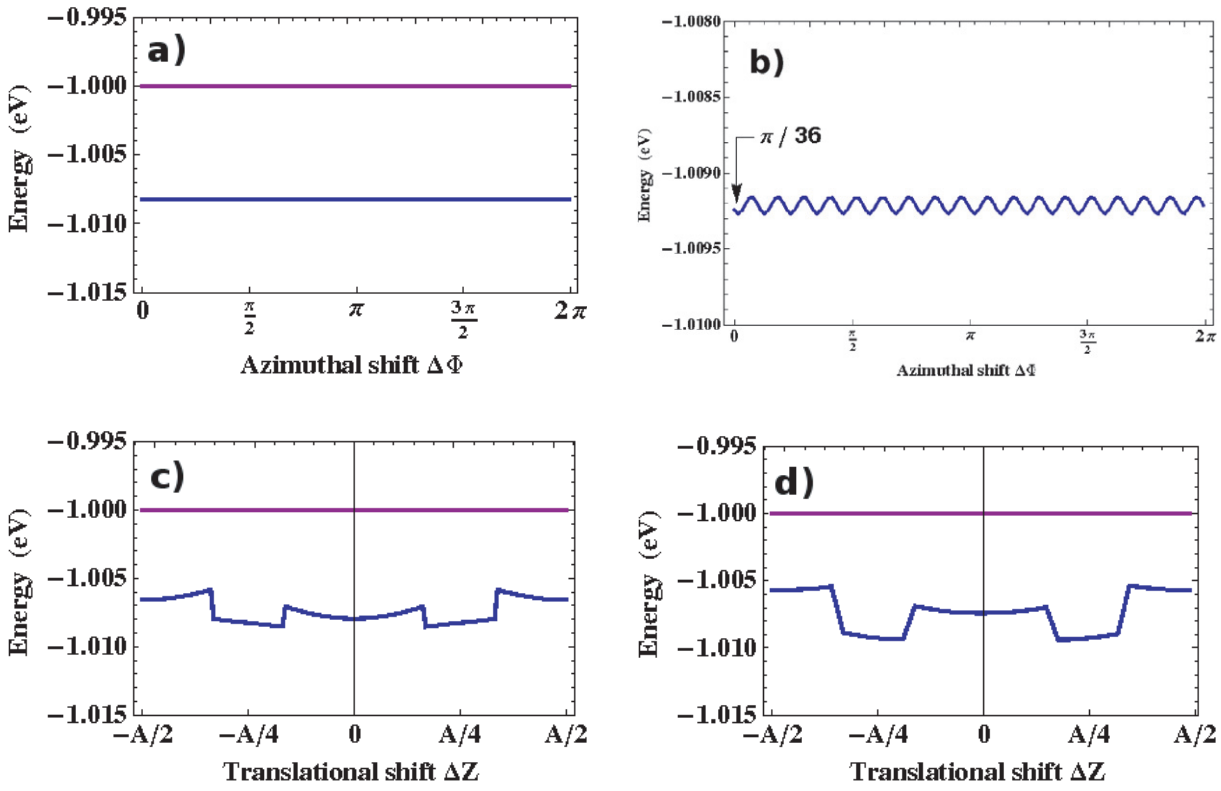

Figure 6. Dependence of total π electronic energy on azimuthal $\Delta\Phi$ (a and b) and translational ΔZ (c and d) for DWNTs $(5, 0)@(14, 0)$ (left panel) and $(9, 0)@(18, 0)$ (right panel) with $\beta_\pi = 1.0\,\text{eV}$ (blue colour). Energy data are normalized to absolute values of the total π electronic energy of the respective non-interacting constituent SWNTs (purple colour).

By inspection of the electronic band structure of figure 5, one can see that the vHs for zigzag DWNTs are still determined by the $k_z = 0$ states in the 1D BZ. One finds that for both DWNT geometries, the azimuthal shift does not affect the DOS structure (not shown), while the translational shifts have a large influence. Figure 7 reports the DOS by changing ΔZ from 0 to $A/4$ together with the DOS spectra of the constituent non-interacting SWNTs. One can see important variations, also at low energies, for both types of DWNTs suggesting that the optical spectra will also have new features with respect to those of the constituent SWNTs. In particular, one observes that also the DOS at $E = 0$, which is constant in the case of the metallic tubes and is calculated as a peak in our calculation due to the finite sampling of the BZ, suffers important changes.

Using the joint DOS (JDOS) and the DWNT eigenvectors, in which the inner and outer tube wavefunctions are mixed due to H_{INTER}, the resulting optical matrix elements are obtained according to the following approximation:

$$M_{z\,\text{DW}}^{\text{opt}} = |\langle\tilde{\Psi}_{\text{DW}}^{c}|\mathbf{P}\cdot\nabla_z|\tilde{\Psi}_{\text{DW}}^{v}\rangle|^2 \approxeq |\langle\tilde{\Psi}_{\text{in}}^{c}|\mathbf{P}\cdot\nabla_z|\tilde{\Psi}_{\text{in}}^{v}\rangle|^2 + |\langle\tilde{\Psi}_{\text{out}}^{c}|\mathbf{P}\cdot\nabla_z|\tilde{\Psi}_{\text{out}}^{v}\rangle|^2. \quad (8)$$

In fact, contributions of mixed type between p_z orbitals belonging to different NTs can be safely ignored due to the fast decay rate of the π orbitals. As a matter of fact, the absolute value of M_{opt} is already very small at a distance of $2a_{\text{CC}}$ and is practically zero at the typical graphitic

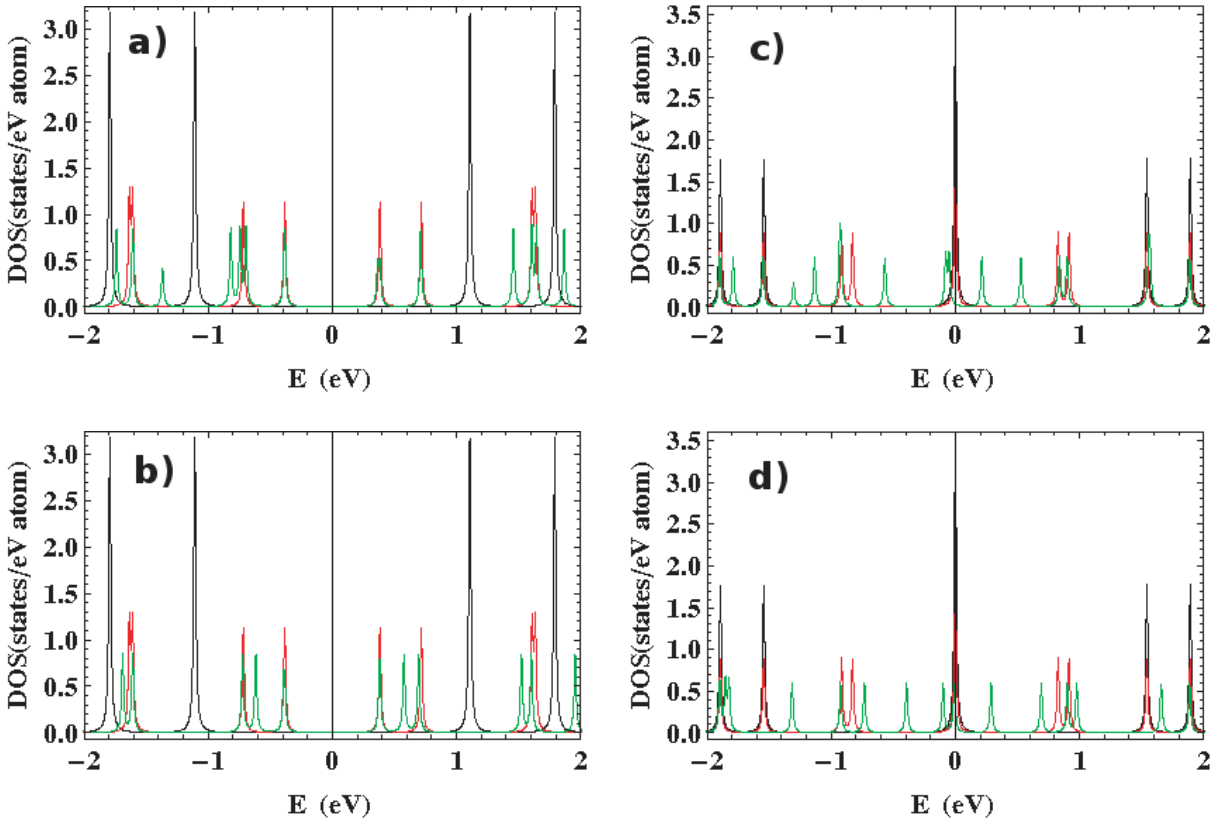

Figure 7. Electronic DOS ($\beta_\pi = 1.0\,\text{eV}$) for (5, 0)@(14, 0) (left panel) with ($\Delta\Phi = 0$, $\Delta Z = 0$) (upper panel) and ($\Delta\Phi = 0$, $\Delta Z = A/4$) (bottom panel). DOS spectra for (9, 0)@(18, 0) (left panel) with ($\Delta\Phi = \pi/36$, $\Delta Z = 0$) (upper panel) and ($\Delta\Phi = \pi/36$, $\Delta Z = A/4$) (bottom panel). Colour legend: inner SWNT (black), outer SWNT (red) and DWNT with intertube interaction (green).

interlayer distance of 0.344 nm for all kinds of molecular orbital configurations [16]. However, new features appear in the spectra due to the new JDOS. The optical absorption intensity can be again calculated for DWNTs employing the SOS method. As noticed for the DOS of both DWNT species, the effect of geometrical parameters on the optical absorption spectra is important when a translational shift ΔZ is considered. Figure 8 shows calculated absorption spectra for the two types of DWNT considered. In general, additional absorption peaks can be found originating from the lifting of the band degeneracies due to the symmetry breaking effect of H_{INTER}. This is particularly evident in the case of the metallic DWNT (9, 0)@(18, 0) for which new bands are observed at low frequencies. For (5, 0)@(14, 0) the lowest peak, corresponding to the E_{11}^S transition of SWNT (14, 0), is poorly affected by the intertube coupling, while new features are found around the E_{22}^S where two peaks are now calculated.

Finally, we also compare the (5, 0)@(14, 0) DWNT optical spectra for three different values of the intertube hopping amplitude (see figure 9), namely $\beta = t_\pi/8$ [43], $\beta = t_\pi/4$ and $\beta = 1.0\,\text{eV}$ [44, 45]. All the observations made above are still valid for the intermediate value $\beta = t_\pi/4$, while for $\beta = t_\pi/8$ only the spectral region above 2.0 eV is visibly affected by the intertube coupling, as shown in figure 10, where a shifted peak related to the inner tube is

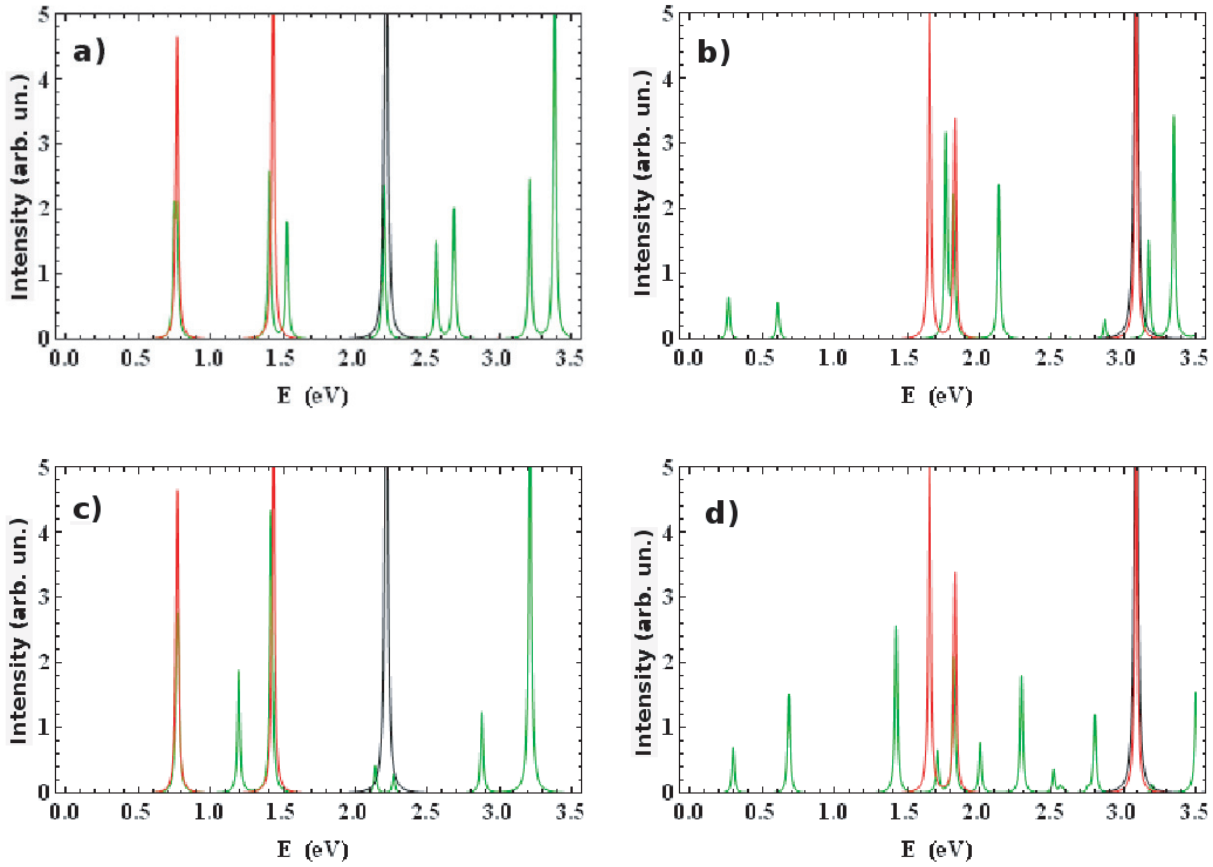

Figure 8. Absorption spectra ($\beta_\pi = 1.0\,\text{eV}$) for (5, 0)@(14, 0) (left panel) with ($\Delta\Phi = 0$, $\Delta Z = 0$) (upper panel) and ($\Delta\Phi = 0$, $\Delta Z = A/4$) (bottom panel). Absorption spectra for (9, 0)@(18, 0) (left panel) with ($\Delta\Phi = \pi/36$, $\Delta Z = 0$) (upper panel) and ($\Delta\Phi = \pi/36$, $\Delta Z = A/4$) (bottom panel). Intensity is given in arbitrary units. Colour legend: inner SWNT (black), outer SWNT (red) and DWNT with intertube interaction (green).

found. Although variations of the spectra can be found for all the values of the intertube hopping parameters a careful evaluation of this parameter must be obtained for appropriate electronic calculations for DWNTs.

One can recall that, on the basis of the hypothesis that the constituent SWNTs are non-interacting units, not all the RBM features have been assigned in the resonance Raman spectra of DWNTs [40, 41]. This is consistent with our results which show that relevant variations of the electronic spectra of both the inner and outer tubes are expected. In particular, some assignments were not possible because the Kataura plot for SWNTs does not show tube resonances at some energies and a tentative assignment based on transitions polarized perpendicular to the NT axis [49] were proposed [41]. Our results show that the interaction between the inner and outer tubes determines a symmetry breaking and new dipole allowed transitions polarized along the NT axis. These new transitions can be used for explaining the Raman assignments. However, a more detailed study of the interlayer hopping integral must be obtained for considering new Kataura plots for DWNTs.

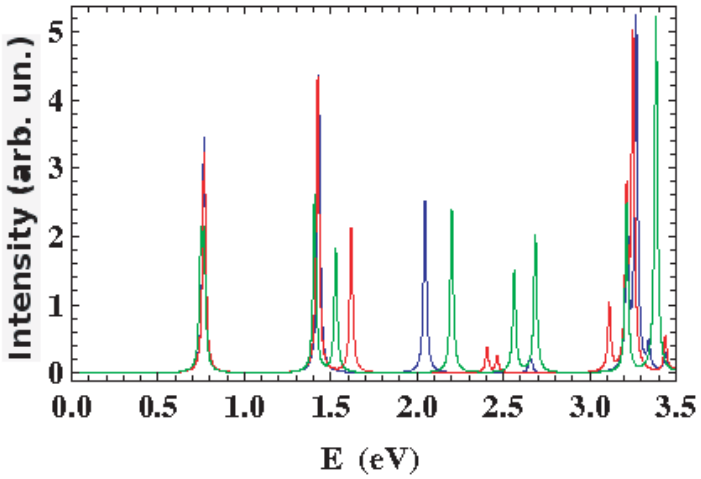

Figure 9. Absorption spectra for (5, 0)@(14, 0) (left panel) with ($\Delta\Phi = 0$, $\Delta Z = 0$) calculated for different values of the intertube hopping parameter β_π. Colour legend: $\beta = t_\pi/8$ (blue), $\beta_\pi = t_\pi/4$ (red) and $\beta_\pi = t_\pi/8 \times 2.75 = 1.0\,\text{eV}$ (green).

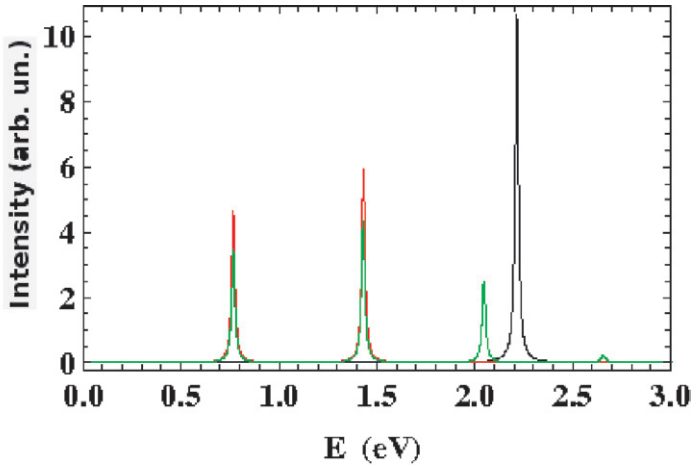

Figure 10. Absorption spectra for (5, 0)@(14, 0) (left) with ($\Delta\Phi = 0$, $\Delta Z = 0$) calculated for non-interacting SWNT constituents ($\beta_\pi = 0\,\text{eV}$) and $\beta_\pi = t_\pi/8$. Colour legend: $\beta = t_\pi/8$ (green), inner SWNT (black) and outer SWNT (red).

4. Conclusion

SCA calculations have been presented for CNTs. We have shown how the appropriate DOS and the optical absorption of the CNTs can be obtained by sampling k points where the vHs are present. The method has been applied to the calculation of the electronic structure of DWNTs with orientation-dependent intertube hopping interactions. The main effect on the electronic structure of the constituent NTs is the appearance of new dipole transition energies originating from the lifting of the band degeneracies due to the symmetry breaking effect of the intertube electronic coupling. The optical spectral features have been shown to be strongly affected particularly by the translational shift parallel to the DWNT axis. Important changes have been

found in the calculated electronic energies of both inner and outer tubes suggesting that revised Kataura plots are needed for the interpretation of experimental data like the resonance Raman spectra of DWNTs. A small number of sites like those considered by the SC approach could be very useful to address other problems relevant for NTs like electronic correlations, and further work is in progress in this direction.

Acknowledgments

Useful correspondence with Professor M Damnjanović, Professor V N Popov, Professor P Lambin, Dr A Grüneis, Dr G Samsonidze and Dr N Nemec is gratefully acknowledged. This work is supported by University of Padova and MIUR (PRIN 2006, Prot. 2006034372).

References

[1] Iijima S 1991 *Nature* **354** 56
[2] Iijima S and Ichihashi T 1993 *Nature* **363** 603
[3] Saito R, Dresselhaus G and Dresselhaus M 1998 *Physical Properties of Carbon Nanotubes* (London: Imperial College Press)
[4] Reich S, Thomsen C and Maultzsch J 2004 *Carbon Nanotubes: Basic Concepts and Physical Properties* (New York: Wiley)
[5] Rao A M *et al* 1997 *Science* **275** 187
[6] Kataura H, Kumazawa Y, Maniwa Y, Umezu I, Suzuki S, Ohtsuka Y and Achiba Y 1999 *Synth. Met.* **103** 2555
[7] Weisman R B and Bachilo S M 2003 *Nano Lett.* **3** 1235
[8] Ando T 1997 *J. Phys. Soc. Japan* **66** 1066
[9] Wang F, Dukovic G, Brus L E and Heinz T F 2005 *Science* **308** 838
[10] Chang E, Bussi G, Ruini A and Molinari E 2004 *Phys. Rev. Lett.* **92** 196401
[11] Perebeinos V, Tersoff J and Avouris P 2004 *Phys. Rev. Lett.* **92** 257402
[12] Spataru C D, Ismail-Beigi S, Benedict L X and Louie S G 2004 *Phys. Rev. Lett.* **92** 077402
[13] Jiang J, Saito R, Samsonidze Ge G, Jorio A, Chou S G, Dresselhaus G and Dresselhaus M S 2007 *Phys. Rev.* B **75** 035407
[14] Capaz R B, Spataru C D, Ismail-Beigi S and Louie S G 2006 *Phys. Rev.* B **74** 121401
[15] Zhao H and Mazumdar S 2004 *Phys. Rev. Lett.* **93** 157402
[16] Samsonidze Ge G 2007 *PhD Thesis* MIT, Boston, MA
[17] Popov V N 2004 *New J. Phys.* **6** 17
[18] Lefebvre J and Finnie P 2008 *Nano Lett.* **8** 1890
[19] Saito R, Dresselhaus G and Dresselhaus M 1993 *J. Appl. Phys.* **73** 494
[20] Liang S-D 2004 *Physica* B **352** 305
[21] Lambin P, Philippe L, Charlier J C and Michenaud J 1994 *Comput. Mater. Sci.* **2** 350
[22] Ho Y H, Chang C P, Shyu F L, Chen R B, Chen S C and Lin M F 2004 *Carbon* **42** 3159
Ho Y H, Ho G W, Chen S C, Ho J H and Lin M F 2007 *Phys. Rev.* B **76** 115422
[23] Charlier J C, Ebbesen T W and Ph. Lambin 1996 *Phys. Rev.* B **53** 11108
[24] Falicov L M 1988 *Recent Progress in Many-body Theories* vol 1 (New York: Plenum) p 275
[25] Meneghetti M 1991 *Phys. Rev.* B **44** 8554
Meneghetti M 1993 *Phys. Rev.* B **47** 13151
Meneghetti M 1994 *Phys. Rev.* B **50** 16899
[26] Dresselhaus M S, Dresselhaus G, Saito R and Jorio A 2005 *Phys. Rep.* **409** 47
[27] Grüneis A 2004 *PhD Thesis* University of Tokyo (chapter 4)

[28] Samsonidze Ge G, Grüneis A, Saito R, Jorio A, Souza Filho A G, Dresselhaus G and Dresselhaus M S 2004 *Phys. Rev.* B **69** 205402
[29] Grüneis A *et al* 2003 *Phys. Rev.* B **67** 165402
[30] Jiang J, Saito R, Grüneis A, Dresselhaus G and Dresselhaus M S 2004 *Carbon* **42** 3169
[31] Malic E, Hirtschulz M, Milde F, Knorr A and Reich S 2006 *Phys. Rev.* B **74** 195431
[32] Hsu H and Reichl L E 2007 *Phys. Rev.* B **76** 045418
[33] Gupta A K, Alon O E and Moiseyev N 2003 *Phys. Rev.* B **68** 205101
[34] Ajiki H and Ando T 1994 *Physica* B **201** 349
[35] Dresselhaus M S and Eklund P C 2000 *Adv. Phys.* **49** 705
[36] Yang X P, Chen J W, Jiang H and Dong J M 2004 *Phys. Rev.* B **69** 193401
[37] Marcolongo G, Ruaro G, Gobbo M and Meneghetti M 2007 *Chem. Commun.* 4925
[38] Kim Y A *et al* 2008 *Appl. Phys. Lett.* **93** 051901
[39] Damnjanović M, Milošević I, Dobardžić E, Vuković T and Nikolić B 2003 *J. Phys. A: Math. Gen.* **36** 10349
[40] Barros E B *et al* 2007 *Phys. Rev.* B **76** 045425
[41] Pfeiffer R, Simon F, Kuzmany H and Popov V N 2005 *Phys. Rev.* B **72** 161404
[42] Hashimoto A, Suenaga K, Urita K, Shimada T, Sugai T, Bandow S, Shinohara H and Iijima S 2005 *Phys. Rev. Lett.* **94** 045504
[43] Roche S, Triozon F, Rubio A and Mayou D 2001 *Phys. Rev.* B **64** 121401
[44] Wang S and Grifoni M 2005 *Phys. Rev. Lett.* **95** 266802
[45] Lu J and Wang S 2007 *Phys. Rev.* B **76** 233103
[46] Charlier J-C, Michenaud J P, Gonze X and Vigneron J-P 1991 *Phys. Rev.* B **44** 13237
[47] Charlier J-C, Michenaud J P and Lambin Ph 1992 *Phys. Rev.* B **46** 4540
[48] Damnjanović M, Dobardžić E, Milošević I, Vuković T and Nikolić B 2003 *New J. Phys.* **5** 148
[49] Grüneis A, Saito R, Jiang J, Samsonidze G G, Pimenta M A, Jorio A, Souza Filho A G, Dresselhaus G and Dresselhaus M S 2004 *Chem. Phys. Lett.* **387** 301